A centroid-based modelling approach to lens inversion for gravitationally lensed systems

Benjamen Smith, Emery Dlugan*

Abstract

In this research, we propose a novel method for determining the coordinate of a gravitational lens in systems where the lens has not yet been directly observed. Our technique uses image processing software to locate the optical centroid of strongly lensed systems and then applies a geometric analysis to derive the coordinates of the lens from the coordinates of the centroid and the arrangement of the lensed images. We demonstrate this method on gravitationally lensed quasar systems in which the lens has been observed to empirically validate our model, and then apply it to the GraL group's list of lensing candidates derived from Gaia DR2[1][2][3] to propose lens coordinates in these candidate systems.

Keywords: quasars, modelling, gravity, gravitational lensing, image processing, lens inversion

Introduction

With the release of Gaia DR2 the search for gravitationally lensed quasar systems has grown. The GraL research group has generated a list of potential candidates for gravitational lensing from the Gaia DR2 data [3], and so begins the work of further investigating each of these systems to determine whether they are indeed instances of gravitational lensing. One of the factors that can be investigated is the presence of a system's lensing object. Unfortunately, no lens has yet been observed in any of the candidate systems proposed by the GraL group. We believe that if the lens coordinates could be precisely predicted for a given system, then attempts at making direct lens observations could be better informed.

For a gravitationally lensed system, the appearance of the system is dictated by parameters describing the locations and properties of the source object and the lens object. In a system with both visible source images and a visible lens, the system can be fully described based on the distances to the lens and source and the angular separations between the visible components. In a system consisting of a bright quasar source and a non-visible lens, it can be difficult to fully describe the system, as without knowing the properties of the lens it is difficult to predict how it affects the light from the source. Lens inversion is a method in which

* Department of Physics and Engineering Physics, College of Arts and Science, University of Saskatchewan, Saskatoon, SK, Canada
Correspondence: **bks512@mail.usask**

University of Saskatchewan Undergraduate Research Journal
Volume 6, Issue 2, 2020

the relevant properties of a lens are sought by analysis of the visible components of the system, and many complex techniques have been applied to this effect [4][5][6].

The basis for our method is the hypothesis that there is a simple geometric relationship between the coordinate of the lens in the system and the coordinate of the luminosity centroid of the lensed source images. For a point-like source (like a quasar) we know this centroid represents the location of the source [7][8]. For a strongly lensed system with a suitably aligned axially symmetric lens object and discrete source images located about an ellipse, we propose that the luminosity centroid is located at a point reflected about both the semi-major and semi-minor axes of the ellipse from the location of the lens, as depicted in Figure 1. As such, by precisely determining the coordinates of the luminosity centroid we should then be able to precisely determine the coordinates of the lens. With the precise coordinates of the lens known, future studies seeking to confirm that the observed system is an instance of gravitational lensing can know at exactly what coordinate the lens is expected to be observed, and so can focus their analysis in seeking a detectable signal in that location. Locating the lens is significant as direct observations of the lens can be used to determine parameters key to fully describing the system.

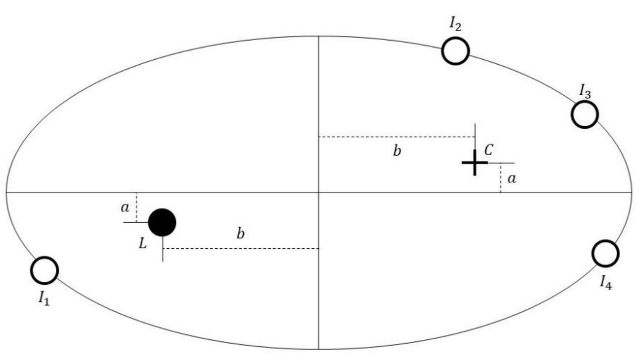

Figure 1: Arrangement of source images, lens object, and centroid in a strongly lensed system. Here, *L* depicts the apparent position of the lens object as seen by an appropriately aligned observer, *C* depicts the position of the luminosity centroid, and I_1 through I_4 depict the lensed source images. The source is not directly visible. The distance from the lens to the semi-major axis is given by *a* and is equal to that distance for the centroid. Similarly, *b* gives the distances to the semi-minor axis from each of the centroid and the lens.

Methodology

Our technique begins with processing images containing the coordinate data for the observed systems. Lacking in .fits files for the systems we aim to analyze, we produce imitation files using Python code to construct an array containing the coordinate data of the actual system. We are using only strongly lensed arrangements to simplify our image reconstruction process. The discrete source images are simpler to simulate as point-like luminosity sources than the continuous luminosity region of weakly lensed ring-like source images.

Our constructed images use Gaia DR2 data on precise coordinates and magnitudes for lensed source images within the system. We plot points representing lensed source images in the array arranged such that the relative separations are consistent with the real system. Our determination of the lensed image centroid requires the lens object not be visible in the image, so by reconstructing only the source images, we can empirically test the efficacy of our algorithm by comparing generated results to known lens coordinates in systems with visible lenses. Furthermore, using real images may introduce obstructing or interfering signals from other sources, which would need to be removed for the software to properly locate the centroid.

In order to locate the elliptic axes, we must draw out the ellipse along which the source images are located. Because there are only four source images in our systems, we are unable to fully describe the ellipse based on the points alone, as at least five points along the boundary are required to unambiguously describe an ellipse. To account for this, we apply a brute-force algorithm to find the center point of the ellipse and assume one of the lensed images is close to the tip of the ellipse so we can calculate the semi-major axis and tilt angle right away. We then locate the center points for which the lensed images share a minor axis length with the smallest possible error and average the ellipse parameters for all fitting ellipses.

We use the AstroImageJ software's single-aperture photometry tool to locate centroids in terms of pixel coordinates on the simulated image. We then propose that by mirroring the centroid coordinates about the semi-major and semi-minor axes, we determine the location of the lensing object, as depicted in Figure 1.

Limitations

As depicted in Figure 1, we construct the ellipse based on the image locations without regarding the lens location. Realistically, an axially symmetric lens object (such as an elliptically shaped galaxy) should always have axes parallel to those of the ellipse along which the images are arranged. We have assumed the furthest source image from the centroid to be the end of the semi-major axis and drawn the most reasonable ellipse based on the brute force centre point determination, and consequently have assumed that the semi-major axis of the lens object is parallel to that of the image ellipse. However, it is not necessarily the case that any

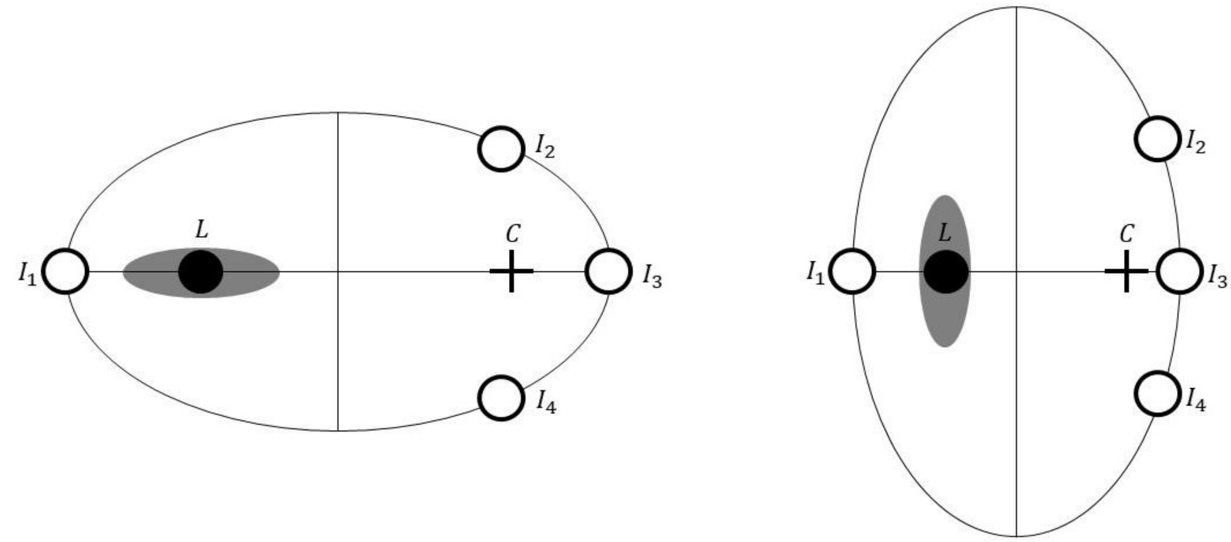

Figure 2: Arrangement of images for two cases of axial alignment in a lensed system. Left: Predicted orientation of images for semi-major alignment. Right: Predicted orientation of images for semi-minor alignment. It is also possible that systems have no clear axial alignment.

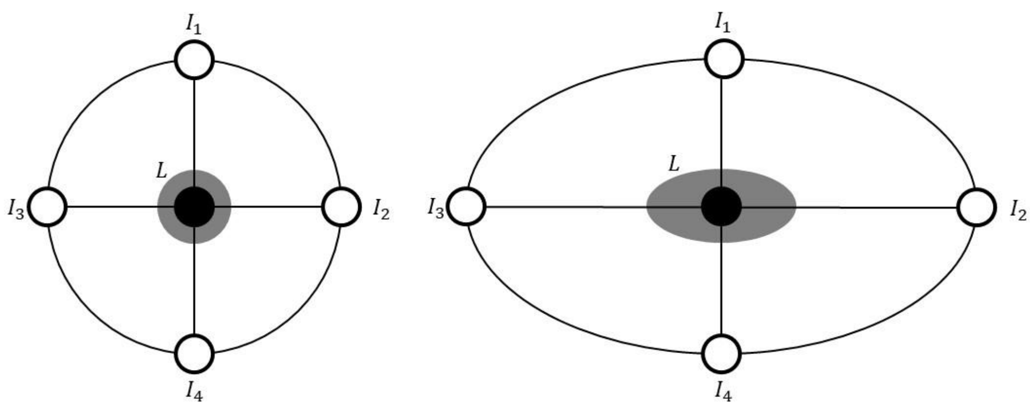

Figure 3: Systems with perfect symmetry where the source and lens are aligned are considered trivial.

image lies exactly on the end of the semi-major axis. For some lensing systems the lens object may be oriented such that an image lies on the semi-minor axis end instead (see Figure 2), or at some angle in between if the lens and source are not axially aligned.

Our algorithm could be built upon such that the ellipse could be drawn for any alignment of the lens axes and source if a more robust parametrization for the ellipse could be found. In short, our program works well for systems in which the source is located near the semimajor alignment of the lens but could be generalized further to work for systems of different alignments as well.

Furthermore, we assume there to be only a single lens object. For a multi-lens system, the image arrangement may not be along the boundary of an ellipse, but along some more complex shape based on the parameters of the collective lensing. For such a system we would not be able to model the lensing with a simple ellipse.

Additionally, our dependence on locating an accurate luminosity centroid means that we cannot apply our algorithm to systems with severely variable luminosity. We have assumed uniform luminosity of the source over time, but any variability will manifest in each of the images separately due to the timing variation between lensed images. Consequently, our method of locating the luminosity centroid will be weighted towards images that have been made brighter by variation. This will prevent the centroid coordinate reflection from accurately locating the lens coordinate. This issue is partially remedied by our regularization of the source images.

For systems where the arrangement of images suggests the source is located at the centre of the ellipse, as in Figure 3, our algorithm will always produce a result placing the lens also at the centre of the system. We consider this to be a trivial case as it does not provide any insight as to the efficacy of our program. This applies both to systems with a circular arrangement of images or to elliptically arranged systems where the images are equally spaced. For this reason, we only selected systems wherein the lens had a visible offset from the centre of the system.

The CASTLES database contains 100 images of gravitationally lensed systems. Due to the present limitations of our algorithm, only systems with non-trivial semi-major alignment are expected to provide meaningful lens coordinate predictions. As such we systematically remove systems for which our algorithm is not applicable.

Our algorithm is most effective for near-circular (but still non-trivial) ellipses. An attempt was made to apply alternative ellipse-fitting methods, including other forms of the ellipse equation, but these approaches produced consistently inferior results. A similar issue occurred while attempting to improve upon the brute-force nature of the code, including incorporating a binary search algorithm in place of the brute-force method. We expect that future research will be able to improve upon our ellipse drawing technique.

Control Tests

To check the efficacy of our model, we will apply it to a series of systems in which the lens has been directly observed. The measurements for the image and lens locations were obtained from the CASTLeS survey [9]. By comparing our predicted lens locations to the observed lens locations, we can determine whether our hypothesis about the relationship between the centroid and lens coordinates is accurate, and what kind of errors are introduced by our assumptions.

Due to the limitations of our algorithm we do not expect to produce valuable results for all systems in the CASTLeS database. Of the 100 systems available, we select 13 systems to produce accurate lens coordinate predictions. We select those systems which appear to have the appropriate symmetry and lens locations that would align with the assumptions of our model. Systems which did not align with our parameters, such as RXJ0911+0551, which has a very counterintuitive apparent lens location clearly not aligned with the theoretical prediction (see Figure 4), produced results with significant error (on the order of 10 times the error of good systems) and so were excluded from the final dataset. We performed cursory tests on systems with trivial symmetry, and as expected produced accurate lens coordinates as expected. Since trivial results are not effective at gauging the efficacy of our algorithm these are excluded from the final dataset. The CASTLeS database also includes multiple systems with no visible images, which were excluded from our testing.

Table 1 shows our testing of the 13 systems for which we expected accurate lens coordinate predictions.

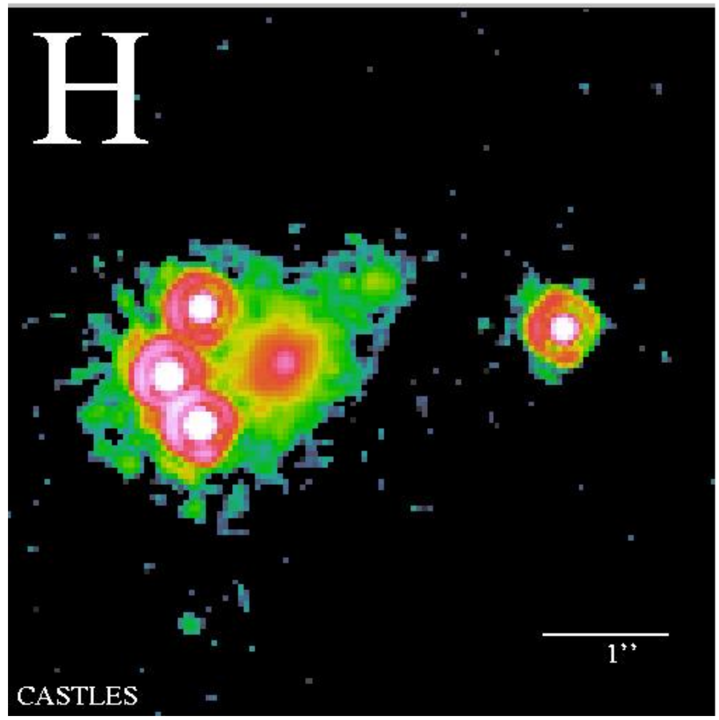

Figure 4: RXJ0911+0551 exhibits an apparent lens placement contradicting the theoretical placement for a general system with elliptical symmetry. The lens appears to be located close to the three closely placed source images on the left, whereas we expect it should be placed nearer to the lone rightmost image.

Application to GraL Candidates

Next, we apply our model to four lensing candidates proposed by the GraL group [3]. As seen in Table 2, our model was able to provide a lens coordinate prediction for one of the GraL group's proposed candidates. We were unable to produce results for the other systems. These other systems had image arrangements that were not arranged along any ellipse our algorithm could produce, and so no lens coordinate prediction could be made. This could be evidence against the candidacy of these systems, but more likely is a limitation of our algorithm following from the assumptions of symmetry we rely on in order to parametrize the ellipse.

Conclusion

From our testing against the CASTLeS data for systems with known lenses, we found that our algorithm is effective at predicting lens locations for systems with approximately

Quasar	True Lens RA	True Lens DEC	Predicted RA	Predicted DEC	Separation (")
SDSS0924+0219	141.2327411	2.323344722	1.41E+02	2.32E+00	0.239175668
Q2237+030	340.1263958	3.358260833	3.40E+02	3.36E+00	0.10813773
HE0230-2130	38.13793667	-21.29025417	38.1380608	-21.29025309	0.446905809
B0712+472	109.0149167	47.14722222	1.09E+02	4.71E+01	0.118288221
HS0810+2554	123.3805419	25.75092861	123.3805667	2.58E+01	0.11140018
PG1115+080	169.5709392	7.765654444	1.70E+02	7.765767407	0.501227147
RXJ1131-1231	172.9645989	-12.53202611	172.9645859	-12.53195625	0.255807982
B1422+231	216.1589144	22.93331778	216.1588103	22.93330361	0.378453674
WFI2026-4536	306.5434299	-45.60774944	3.07E+02	-45.60767167	0.318660257
WFI2033-4723	308.4249339	-46.60463667	308.4250678	-4.66E+01	0.488111668
H1413+117	213.9433728	11.49498917	2.14E+02	1.15E+01	0.038013156
HE0435-1223	69.56175972	-11.71282583	69.56175741	-1.17E+01	0.083417291
SDSS1138+0314	174.515285	3.249592778	174.5152639	3.25E+00	0.079120162

Table 1: Comparing known lens coordinates to lens coordinates measured from our centroid model. Right ascension and declination values are given in degrees (°). The angular separation between measured and actual lens location is given in arcseconds (").

semi-major alignment within a reasonable margin of error (δ = 0.24"). Our program behaved as expected for all tested systems, including trivial and fail cases. We were then able to make predictions about the lens location in the tested GraL candidate system (Table 2).

The system 11310013-1149559935 has been observed to have a timing variation indicative of gravitational lensing [10]. Our data then agrees well with this additional evidence, as we have demonstrated this system has geometric properties consistent with lensing. This instance demonstrates that our algorithm is effective at predicting the lensing nature in the systems for which its assumptions about symmetry and alignment are accurate. We believe this technique could be applied as a criterion to be used in data mining of Gaia DR2 when searching for gravitational lensing candidate systems.

Quasar	Predicted RA	Predicted DEC
113100013-441959935	172.7499378	-44.33338633

Table 2: The predicted lens coordinates for GraL lensing candidate system. The right ascension and declination values are given in degrees (°).

Acknowledgements

This work has made use of data from the European Space Agency (ESA) mission Gaia (https://www.cosmos.esa.int/gaia), processed by the Gaia Data Processing and Analysis Consortium (DPAC, https://www.cosmos.esa.int/web/gaia/dpac/consortium). Funding for the DPAC has been provided by national institutions, in particular the institutions participating in the Gaia Multilateral Agreement.

This work also made use of the following software: SciPy [11], PyCharm [12], NumPy [13], Astropy [14], and AstroImageJ [15].

References

1. T. Prusti et al. Gaia Collaboration, Astronomy and Astrophysics, **595**, A1 (2016).

2. A. G. A. Brown et al. Gaia Collaboration, Astronomy and Astrophysics, **616**, A1 (2018).

3. L. Delchambre et al. Astronomy and Astrophysics, **622**, A165 (2019).

4. B. Brewer and G. Lewis, Publications of the Astronomical Society of Australia, **22**(2), 128 (2005).

5. B. Brewer and G. Lewis, The Astrophysical Journal, **637**(2), 608 (2006).

6. R. Joseph, F. Courbin, J. –L. Starck, and S. Birrer, Astronomy and Astrophysics, **623**, A14 (2019).

7. S. H. Suyu, P. J. Marshall, M. P. Hobson, and R. D. Blandford. Monthly Notices of the Royal Astronomical Society, **371**(2), (2006).

8. A. Tagore and C. Keeton, Monthly Notices of the Royal Astronomical Society, **445**(1), 694 (2014).

9. C. S. Kochanek et al. Castles survey, https://www.cfa.harvard.edu/castles/, Accessed online: November 28th 2018.

10. O. Wertz et al. Gaia GraL, Astronomy and Astrophysics, **628,** A17 (2019).

11. E. Jones et al. computer code SciPy, http://www.scipy.org/, accessed online August 16th 2018, (2001).

12. JetBrains, computer code PyCharm. https://www.jetbrains.com/pycharm/, accessed online August 16th 2018, (2017).

13. T. E. Oliphant, *A guide to NumPy* (Trelgol Publishing USA, 2006), Vol 1.

14. T. P. Robitaille et al. Astronomy and Astrophysics, **558**, A33 (2013).

15. K. Collins and J. Kielkopf, Astrophysics Source Code Library (2013).